Energy 338 (2025) 138628

Contents lists available at ScienceDirect

Energy

journal homepage: www.elsevier.com/locate/energy

Optimal decarbonization of urban heating systems considering interdependencies between building retrofits and heat supplies

Carolin Ayasse *, Julia Barbosa, Florian Steinke

Energy Information Networks and Systems, Technical University of Darmstadt, Landgraf-Georg-Str. 4, Darmstadt, 64283, Hessen, Germany

ARTICLE INFO

Keywords:
Energy system model
District heating
Building retrofit
Decarbonization
Mixed-integer linear programming

ABSTRACT

Optimal decarbonization paths of urban heating systems contain both heat demand- and supply-side related measures. Building retrofits, i.e., measures that increase buildings' energy efficiency, affect the optimal choice of heat generation, which in turn influences optimal building retrofit decisions. Existing energy system models struggle to represent these interdependencies model-endogenously; either a high level of abstraction does not capture key characteristics of the heating system sufficiently accurately or the computational costs are too high if existing, detailed methods are applied at an urban scale. This paper presents mixed-integer linear programming-style optimization conditions that allow to treat these interdependencies model-endogenously at an urban scale with a heterogeneous residential building stock. The urban area is divided into districts, each with multiple archetype buildings representing various building types and energy standards. Retrofit decisions are determined within the model for each district, reducing heat demands and enabling lower heat supply temperatures and thereby more efficient heat generation units. Different existing mixed-integer linear programming-based energy system modeling frameworks can be extended using the proposed new conditions, with only five coupling constraints to the remainder of the system. The technical benefits of the methodology are demonstrated with an experimental case study featuring an urban area with three districts.

1. Introduction

Decarbonizing the heat supply of buildings is essential for achieving energy and climate targets [1]. Currently, 75% of buildings in the European Union are energy-inefficient, and 50% of residential space heating relies on natural gas or oil [2]. Addressing these challenges at the level of individual buildings is insufficient, as solutions like district heating networks (DHNs) operate on scales larger than a single building [3]. District heating offers significant potential for reducing primary energy use in the European Union [4]. Consequently, research shifted towards approaches that consider entire districts or even larger spatial scales. The adoption of 4th Generation District Heating systems (4GDHs) [5], which integrate renewable energy sources and operate at lower supply temperatures, requires additional accounting for building retrofits, such as adding insulation to individual building components, to reduce the total heat demand [6].

Partial equilibrium energy system models are widely used for the techno-economic optimization at various scales. Multiple frameworks for energy system modeling (ESM) such as TIMES [7], OSeMOSYS [8], oemof [9] or CESM [10] share a similar abstraction level, encompassing energy carriers and transformation processes. However, if applied to the heating sector at an urban scale, they fail to represent key characteristics sufficiently accurately. There exist complex interdependencies between heat demand-side and heat supply-side measures [11], and they should therefore be considered simultaneously [12]. For example, after retrofitting the building envelope, the heat supply temperature can be lowered, and as a consequence the efficiency of an installed heat pump (HP) increases. Buildings can either have their own individual heat generation unit (HGUB), or receive heat from a locally available DHN supplied by various central heat generation units (HGUCs). Municipal policymakers and local energy providers have to decide where to develop DHNs and where to prioritize individual heating systems. To support this decision-making process, energy system models must be able to account for local factors, such as a heterogeneous building stock, zoning regulations, or the proximity and availability of heat sources, e.g., a waste heat source. All these requirements make the planning task complex and there exists a trade-off between computational costs and representation of individual building characteristics [13].

* Corresponding author.
E-mail address: carolin.ayasse@eins.tu-darmstadt.de (C. Ayasse).

https://doi.org/10.1016/j.energy.2025.138628
Received 23 May 2025; Received in revised form 11 September 2025; Accepted 21 September 2025
Available online 27 September 2025

Nomenclature

Sets

$\mathcal{A}$	archetype building (a)
$\mathcal{C}$	conversion process (c)
$\mathcal{D}$	district (d)
$\mathcal{H}$	individual heat generation unit (HGUB) (h)
$\mathcal{T}$	time step of an investment year (t)
Θ	temperature of a DHN (θ)
$\mathcal{Y}$	investment year (y)
Γ	mapping c to HGUCs which supply θ (c, θ)
Ω	mapping c to HGUBs which require θ (c, θ)
Υ	mapping c to demand of buildings (c, a)
Ψ	mapping c to HGUBs (c, h)

Variables

$CAPEX$	capital expenditures
$e^{\text{outtime}}_{c,t,y,d}$	energy output per time step
$e^{\text{outtot}}_{c,y,d}$	total energy output per year
$GENEX$	HGUBs expenditures
$n^{\text{B}}_{a,y,d}$	number of buildings per archetype
$n^{\text{G}}_{h,a^{\text{I}},y,d}$	number of HGUBs initially installed in a^{I}
$n^{\text{G}}_{h,a^{\text{I}},a^{\text{OP}},y,d}$	number of HGUBs operating in a^{OP}
$n^{\text{G,new}}_{h,a^{\text{I}},y,d}$	number of newly built HGUBs
$OPEX$	operational expenditures
$p^{\text{max}}_{c,y,d}$	installed capacity
$RETEX$	building retrofit expenditures
$TOTEX$	total expenditures
$u_{\theta,y,d}$	binary indicating the temperature of a DHN
v^{B}	total salvage value of building retrofits
$v^{\text{B}}_{a\to a',y,d}$	discounted salvage value of building retrofits
v^{C}	total salvage value of conversion processes
v^{G}	total salvage value of HGUBs
$v^{\text{G}}_{h,a^{\text{I}},y,d}$	discounted salvage value of HGUBs
$\Delta n^{\text{B}}_{a\to a',y,d}$	number of building retrofits $a \to a'$
$\Delta n^{\text{G}}_{h,a^{\text{I}},a\to a',y,d}$	number of retrofits $a \to a'$ with h which were initially installed in a^{I}

Parameters

$D_{a,y,d}$	heat demand
$E^{\text{outtot}}_{c,y,d}$	total yearly energy output
F_y	discount factor
$K^{\text{B}}_{a\to a',d}$	building retrofit costs
$K^{\text{G}}_{h,a^{\text{I}},y,d}$	HGUB costs
L^{G}_{h}	technical lifetime of HGUBs
$L^{\text{B}}_{a\to a'}$	building retrofit lifetime
M	big-M constant
N^{B}_{d}	total number of buildings
$N^{\text{B}}_{a,y_0,d}$	number of buildings per archetype
$N^{\text{G,res}}_{h,a^{\text{I}},y,d}$	residual number of HGUBs
$P_{c,t,d}$	load shape of energy output
$\Delta\overline{N}^{\text{B}}$	maximum retrofit rate of the urban area
$\Delta\underline{N}^{\text{B}}$	minimum retrofit rate of the urban area

1.1. Literature

The decarbonization of urban heating systems can be approached in different ways. The literature is categorized as (i) geographical information system (GIS) analysis, (ii) simulation-based approaches, (iii) optimization-based methods, relying on algorithms without optimality guarantee, and (iv) optimization-based methods which provide globally optimal solutions, particularly mixed-integer linear programming (MILP).

(i) In practice, heat planning for urban areas is often based on predominantly manual GIS analysis. A common method for identifying potential areas for DHNs involves using the linear heat density, defined as the annual heat demand per meter of grid length [14]. (ii) Simulation-based approaches focus on accurately representing systems and projecting future scenarios rather than finding an optimal solution. For instance, [15] use EnergyPlan [16] to simulate Beijing's heating systems until 2030, while [17] apply agent-based modeling to simulate retrofit adoption in neighborhoods over 20 years.

(iii) Optimization-based approaches use algorithms to minimize a predefined objective function. Heuristic optimization algorithms can handle large, complex problems but do not guarantee global optimality [18]. Co-simulation methods combine optimization with detailed modeling. For example, [19] couple metaheuristics with EnergyPlus [20], and [21] integrate metaheuristics with MILP. In [22], EnergyPlus is used iteratively to predict heat demand under various retrofit scenarios, with retrofit measure selection guided by designer experience. The authors of [23] employ artificial neural networks and surrogate models to identify near-optimal retrofit solutions.

(iv) Since for energy system planning the possible design space is huge, it is valuable to employ algorithms that can provide provable global optimality guarantees, even if that comes at reduced modeling detail to ensure feasible solving times. In heat planning, this often involves solving (MI)LPs. The authors of [24] formulate a MILP to examine optimal district-level decarbonization strategies, where building retrofit decisions are made exogenously, that is, they are predefined and provided as an input to the model, thus limiting flexibility. In contrast, [25,26] present MILP-based frameworks that model supply–demand interdependencies endogenously, allowing the model to decide on retrofits using multiple binary variables per building. While this provides a detailed representation of the heating sector, it is not suitable for application to large urban areas due to high computational costs of using multiple binary variables for each building.

To reduce computational costs at urban scales, various studies employ clustering and archetype buildings. In [27] the authors focus on DHNs sizing and operation, without considering individual heat supply. [28] include individual heat supply in the reference scenario but do not endogenously capture trade-offs between individual heat supply and DHN. Meanwhile, [13] model supply–demand interdependencies for individual buildings, without addressing DHNs. All three studies focus on a single district, lacking further spatial resolution. In contrast, the authors of [29] define spatial nodes with one archetype building per district to optimize demand and supply strategies. In [30], clustering is used to define representative buildings and districts for modeling Switzerland's entire building stock. The spatial resolution remains relatively coarse, encompassing entire communities without further division within those communities.

The presented literature reveals that numerous studies explore optimal decarbonization pathways for urban heating systems. However, a research gap remains for an optimization-based methodology that combines important model quality criteria (i–iv) with sufficient computational performance (v,vi). Specifically, there is a need for a methodology that (i) accurately models interdependencies between heat supply and heat demand model-endogenously, (ii) can include both DHNs and individual heat supply systems, can be (iii) spatially resolved, with (iv) multiple archetype buildings per district, and (v) is applicable on urban scales while (vi) relying on solution algorithms which provide provable global optimality guarantees.

1.2. Contribution

This paper proposes a set of novel MILP-style conditions to endogenously model interdependencies between heat supply and retrofit measures at urban scales. They can be used together with various existing MILP ESM frameworks with low adaption effort. The approach extends existing literature by allowing for (i) endogenous modeling of interdependencies between heat supply and retrofit measures at high accuracy, particularly the interdependencies between retrofit measures, the technical suitability of specific HGUBs, and the efficiency of the HGUBs. (ii) It considers both DHNs and individual heat supply systems and is (iii) spatially resolved, along with the definition of (iv) multiple archetype buildings per district. The formulation as a MILP with a limited number of integers ensures (v) scalability to urban scales and (vi) optimality guarantees.

The proposed conditions are designed for urban-scale applications with a heterogeneous building stock. An urban area is divided into various districts to identify potential areas for DHNs and includes multiple investment years to accommodate long planning horizons. To balance scalability and accurate heating sector representation, multiple archetype buildings per district are defined, with archetypes representing various building types and different energy standards of these. The definition of archetype buildings mainly refers to the demand-side. The optimal heat supply of buildings can differ across and within archetypes. The conditions integrate into different existing ESM frameworks via five coupling constraints.

The case study shows that optimizing retrofit decisions together with the heating system model-endogenously, under the proposed conditions, helps to identify cost-saving potentials compared to separate planning. For instance, it can affect decisions on where to connect buildings to a DHN and where to retrofit buildings.

The remainder of this paper is structured as follows: In Section 2 an abstract model of common ESM frameworks is introduced and its limitations with respect to the clustering of buildings, the aggregation of demands, and building retrofits are discussed. In Section 3 the proposed novel MILP-conditions are introduced. A case study is presented in Section 4 and the paper concludes in Section 5.

2. Existing energy system modeling frameworks and their limitations

This section introduces key concepts of partial equilibrium ESM optimization frameworks like TIMES [7], OSeMOSYS [8], oemof [9] or CESM [10], which, while differing in terminology, share similar abstractions. These abstractions are outlined using the terminology and structure of the CESM framework [10] which is used as a basis for this work. Furthermore, limitations of this type of models when examining retrofits and when aggregating heat demands and HGUBs are addressed.

2.1. Abstractions and notation

The targeted energy system models consist of *energy commodities* $m \in \mathcal{M}$, such as natural gas, electricity, or heat, and *conversion processes* $c \in C$ which transform one energy commodity into another, e.g., heat-only boilers (HOBs) converting natural gas into heat. This abstraction can cover multi-input and multi-output conversion processes. The models typically cover multiple investment years $y \in \mathcal{Y}$, each represented via multiple time steps $t \in \mathcal{T}$. Conversion processes are characterized by their capacity and energy throughput per time step, along with technical aspects such as efficiency and costs. Energy balance constraints ensure equality between the supply and demand of each energy commodity. Exogenous commodities are used to describe energy forms outside the model boundaries, and are used to describe imports of energy into the model as well as energy demands. Emission constraints can be used to limit emissions to an annual emission cap. Table 1 shows the correspondence of the introduced concepts between the CESM and OSeMOSYS framework.

Table 1
Terminology of corresponding abstractions in CESM and OSeMOSYS.

CESM [10]	OSeMOSYS [8]
commodity	fuel
conversion process	technology
conversion process from	technology without input
exogenous commodity	activity
conversion process to	demand
exogenous commodity	
year	year
time step	time slice
yearly energy output of	total annual activity of
conversion process	technology
efficiency	output activity ratio/input activity ratio

For this work, the original CESM [10] framework is extended as follows: district-specific modeling is incorporated by adding an index for a district $d \in D$ to all quantities. Additional transport conversion processes enable energy transport between districts. Moreover, capacity-independent investment costs are introduced, that apply whenever the newly installed capacity of a conversion process is larger than zero. This extension transforms the original linear programming (LP) formulation into a MILP problem.

Throughout the paper, variables are denoted by lowercase letters, while parameters are represented by uppercase letters. Indices are assumed to belong to the sets given at their first appearance, unless otherwise specified.

2.2. Limitations

When modeling energy systems at urban scales, multiple HGUBs as well as multiple demands are commonly aggregated to reduce computational costs. This comes with the loss of a one-to-one assignment of heat demands to HGUBs and can lead to an oversimplification of diverse characteristics of the building sector as detailed in the following.

False representation of capacities. If multiple HGUBs of the same type are aggregated into one virtual HGUB this may lead to a skewing of required capacities, if the virtual HGUB serves multiple buildings with different heat demand profiles.

To illustrate this shortcoming, assume a model structure as in Fig. 1a, implemented with the above described ESM framework. In Fig. 1b individual heat demands of two buildings and their combined demand are plotted. The required heating capacities are 3.00 kW for building 1 and 3.50 kW for building 2. Due to non-simultaneous load peaks, a joint HGUB supplying the aggregated demands would require a heating capacity of only 5.47 kW, underestimating the actual need of 6.5 kW by 16 %. This misrepresentation affects investment cost calculations which rely on installed capacities.

Cooperation of individual heat generation units. The naive aggregation of demands and HGUBs can lead to unrealistic cooperation among HGUBs. If the model structure in Fig. 1a is modeled naively, the resulting heat supply structure may resemble that shown in Fig. 1c. In this scenario, the HP supplies heat to both buildings during low electricity price periods, while the HOB operates for the remainder of the day. This setup contradicts the assumption that, with individual heat supply, HGUBs serve only the buildings in which they are installed.

To account for that, the following constraints can be imposed: (i) the shape of a HGUB's energy output is required to match the demand profile of the building it serves, and (ii) the yearly energy output of a HGUB must correspond to the heat demand of the building it serves.

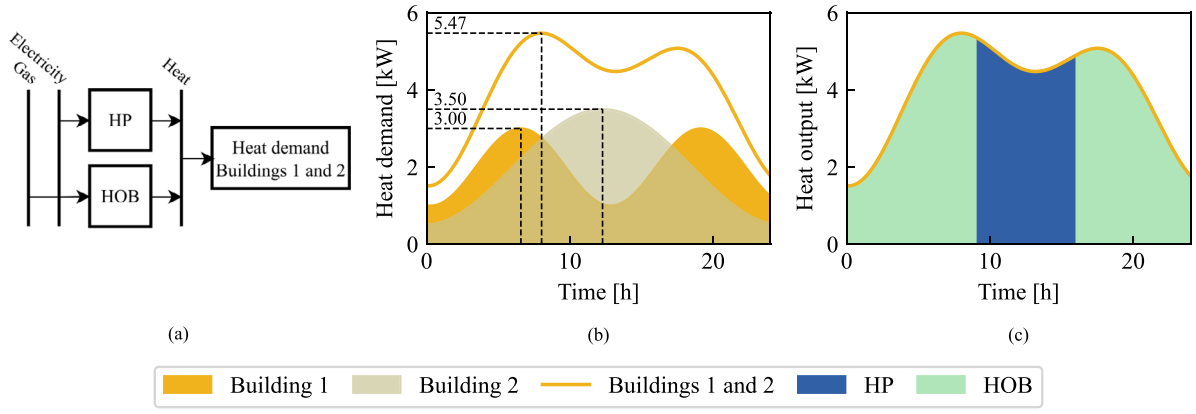

Fig. 1. Limitations of ESM frameworks when aggregating supply and demand. (a) Possible model structure in heat planning. Commodities are represented by vertical lines and conversion processes are represented by rectangles. (b) False representation of required heating capacity. (c) Cooperation of HGUBs to meet the total heat demand.

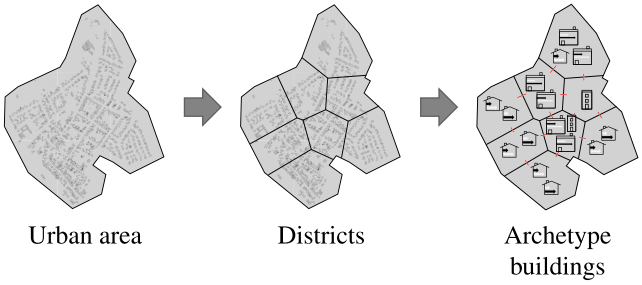

Fig. 2. An urban area is divided into multiple districts. For each district, multiple archetype buildings are defined. DHNs of neighboring districts can be interconnected.

Specifically, to model (i), let $e^{\text{outtot}}_{c,y,d}$ be the energy output of a conversion process c in year y and district d. The energy output in one time step t is $e^{\text{outtime}}_{c,t,y,d}$ and can be constrained by

$$e^{\text{outtime}}_{c,t,y,d} = P_{c,t,d} e^{\text{outtot}}_{c,y,d}, \quad \forall c, t, y, d, \tag{1}$$

with $P_{c,t,d}$ denoting the predefined load profile as the proportion of energy output during a time step relative to the total yearly energy output, i.e., $\sum_t P_{c,t,d} = 1$ [31].

With respect to (ii), let $E^{\text{outtot}}_{c,y,d}$ be the predefined energy output of a conversion process. The energy output of a conversion process is constrained as

$$e^{\text{outtot}}_{c,y,d} = E^{\text{outtot}}_{c,y,d}, \quad \forall c, y, d, \tag{2}$$

where $E^{\text{outtot}}_{c,y,d}$ is the yearly heat demand of the building a HGUB supplies.

While (i) and (ii) are sufficient when building retrofits are not considered, they cannot be updated endogenously to reflect the building's heat demand after retrofitting within existing ESM frameworks. Without updating, the capacity of one installed HGUB might suffice to provide heat to multiple buildings.

3. The proposed retrofit optimization conditions

This section outlines the proposed approach to enhance existing ESM frameworks to improve the modeling of interdependencies between heat supply-side and demand-side measures at an urban scale and to overcome the limitations specified in the previous section. The proposed approach involves extending an existing energy system model with the additional, novel conditions. Given a multimodal energy system model of an urban area this paper proposes to remodel the individual heating sector and DHNs. The proposed novel conditions are based on optimizing for every investment year the *number of buildings* in a district that (i) are of a certain archetype and (ii) the number of HGUBs in such buildings.

All buildings are assumed to belong to an *archetype* $a \in \mathcal{A}$. Archetypes can represent different building types as well as different energy standards of these. They are characterized by a predefined heat demand with a fixed time profile. Building retrofit is modeled as the change of a building from one archetype a to another archetype a', possibly via multiple steps, and is denoted as $a \to a'$. This implies a strict partial order on the set of archetypes representing all possible retrofit pathways. Therefore, the number of buildings per archetype is an optimization variable and changes over time through building retrofit. The heating system in each building is modeled independently of the archetype. Each building is assumed to have exactly one HGUB out of a set of options $h \in \mathcal{H}$, e.g., a HP or a HOB. An urban area is divided into multiple districts, each featuring a specific mix of archetype buildings, see Fig. 2. Districts should be defined to group buildings with similar characteristics, thereby minimizing the number of archetype buildings to be considered within each district. They should capture local heating system characteristics, such as HP restrictions in dense urban areas or the availability of heat sources.

3.1. Setup within existing energy system modeling framework

Fig. 3 illustrates how the heating system has to be set up with an existing ESM framework, while other model parts are not affected. A distinct heat demand conversion process has to be defined for every archetype a, with each heat demand aggregating the heating needs of all buildings of one archetype.

For the individual heating systems, there exists a conversion process for every type of HGUB h supplying an archetype a. For example, a distinct conversion process is modeled for each archetype a a HP supplies within a district d. Distinct energy efficiencies can be indicated for HGUBs, depending on the supplied archetype. For example, the efficiency of a HP can improve with the energy standard of the archetype building. To avoid cooperation of HGUBs, their heat output load shape is constrained by Eq. (1) to match exactly the load shape of the supplied archetype. Costs for the installation of a new HGUB are not assigned to the conversion processes of the ESM framework but instead depend on the *number* of installed HGUBs in a district as described in Section 3.2.

DHNs at different temperatures $\theta \in \Theta$ are defined as distinct conversion processes, each characterized by individual efficiencies. DHNs operating at lower temperatures can therefore have lower losses compared to those operating at higher temperatures. Investment costs are not directly assigned to the DHN of a certain temperature, but

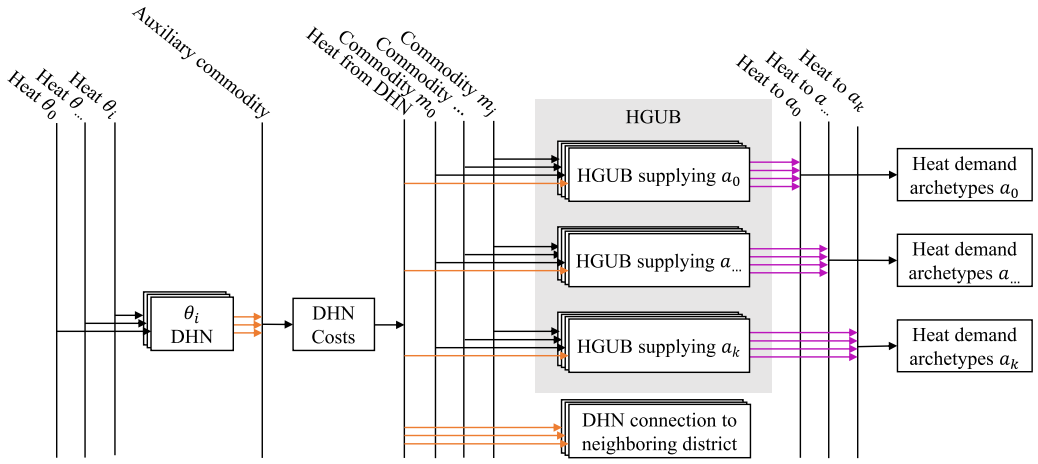

Fig. 3. Special structure of an energy system model considering the parts which are affected by the conditions presented in this work. Vertical lines represent commodities and rectangles represent conversion processes. The load shape of energy flows highlighted purple is constrained according to Eq. (1). Energy flows highlighted orange are constrained depending on the temperature of the DHN (Eqs. (22) and (23)).

depend on auxiliary conversion processes *DHN Costs* for each district. This approach allows the temperature of a DHN to decrease over time as building retrofits reduce heat demand, without necessitating investments in a new DHN. Based on binary variables capacity-independent investment costs are assigned to the auxiliary process *DHN Costs*, reflecting the high upfront construction expenses of developing a new DHN in a district, compared to the lower costs of connecting additional buildings. The binary variable $u_{\theta,y,d}$ indicates whether a DHN operates at temperature θ. The temperature of the DHN imposes constraints on certain energy flows to and from the network. The heat exchanger to connect a building to a DHN is modeled as a HGUB, using heat from the DHN as the input commodity after accounting for distribution losses.

3.2. New conditions modeling the number of instances

The following section describes the novel conditions centered around the number of buildings and HGUBs within a year y and district d. Let $n^{\mathrm{B}}_{a,y,d}$ denote the number of buildings per archetype a, district d, and year y. The total number of buildings undergoing retrofit $a \to a'$ is $\Delta n^{\mathrm{B}}_{a\to a',y,d}$. Regarding the number of HGUBs installed in buildings, the model distinguishes between the archetype a^{I}, which corresponds to the building's archetype at the time the HGUB was initially installed, and the archetype a^{OP}, which indicates the archetype of the building where the HGUB currently operates. A difference between a^{I} and a^{OP} may occur if a building is retrofitted without replacing the existing HGUB. Let $n^{\mathrm{G}}_{h,a^{\mathrm{I}},y,d}$ denote the number of HGUBs installed in buildings of archetype a^{I}, in year y and district d. This number depends on both the residual number of HGUBs, $N^{\mathrm{G,res}}_{h,a^{\mathrm{I}},y,d}$, from before the modeling period, and the number of newly built HGUBs, $n^{\mathrm{G,new}}_{h,a^{\mathrm{I}},y,d}$. The variable $n^{\mathrm{G}}_{h,a^{\mathrm{I}},a^{\mathrm{OP}},y,d}$ additionally specifies the archetype of the buildings where the HGUBs operate. If a building, in which a HGUB was initially installed under archetype a^{I}, is retrofitted according to $a \to a'$ without replacing the HGUB, this is indicated by $\Delta n^{\mathrm{G}}_{h,a^{\mathrm{I}},a\to a',y,d}$.

Fig. 4 provides a visualization of all variables indicating the number of buildings or HGUBs. Note that these variables are chosen to be continuous for computational efficiency reasons. Hence, the optimization may yield fractional values which implies a certain model error compared to realistic integer decisions. This discretization error can be reduced by choosing large enough districts. The relevance of the remaining errors should then be evaluated relative to other uncertainties and possible error sources in the model. If, for instance, one assumes an accuracy of the demand and costs forecasts in the range of 10 %, then a minimum of 10 buildings of each archetype supplied by a certain HGUB should ensure that the discretization errors are not dominating.

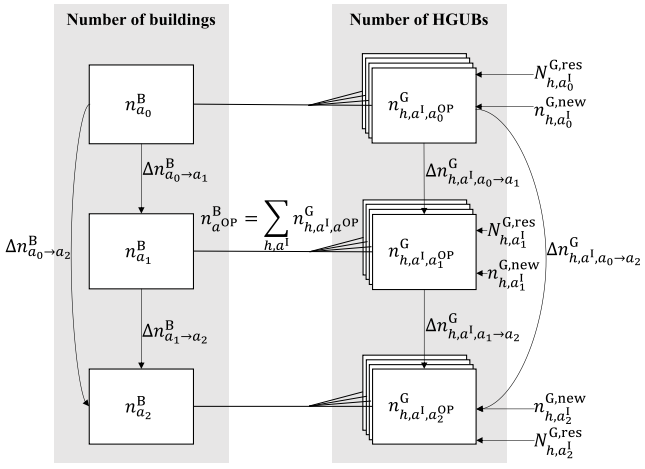

Fig. 4. Overview of the number-based variables for one year in a district with three archetype buildings, representing energy standards from lowest a_0 to highest a_2.

3.2.1. Number of buildings

The sum of all buildings per archetype $n^{\mathrm{B}}_{a,y,d}$ has to match the district's total number of buildings N^{B}_{d}, i.e.,

$$\sum_{a} n^{\mathrm{B}}_{a,y,d} = N^{\mathrm{B}}_{d}, \quad \forall y, d. \tag{3}$$

The number of buildings per archetype and district in the first year of the modeling period y_0 is denoted by $N^{\mathrm{B}}_{a,y_0,d}$, so that

$$n^{\mathrm{B}}_{a,y_0,d} = N^{\mathrm{B}}_{a,y_0,d}, \quad \forall a, d. \tag{4}$$

The number of buildings which are retrofitted in one year and district is $\Delta n^{\mathrm{B}}_{a\to a',y,d}$. Note that, while the number of retrofitted buildings is continuous, the retrofit measures themselves are discrete and defined by the strict partial order imposed on the set of archetypes $\mathcal{A}$. The total number of building retrofits within the urban area is limited by

$$\underline{\Delta N}^{\mathrm{B}} \le \sum_{a\to a',d} \Delta n^{\mathrm{B}}_{a\to a',y,d} \le \overline{\Delta N}^{\mathrm{B}}, \quad \forall y, \tag{5}$$

where $\underline{\Delta N}^{\mathrm{B}}$ and $\overline{\Delta N}^{\mathrm{B}}$ define minimum and maximum retrofit rates in total number of buildings for the whole urban area. The number of

buildings per archetype changes over the modeling period as

$$n^{\mathrm{B}}_{a,y,d} = n^{\mathrm{B}}_{a,y-1,d} + \sum_{\substack{a' \\ a'\to a}} \Delta n^{\mathrm{B}}_{a'\to a,y,d} - \sum_{\substack{a' \\ a\to a'}} \Delta n^{\mathrm{B}}_{a\to a',y,d}, \quad \forall a,y,d, \quad \text{if } y > y_0. \tag{6}$$

This equation does not account for new construction or building demolition, though these factors could be easily included. The costs of retrofit $a \to a'$ in a district d are denoted by $K^{\mathrm{B}}_{a\to a',d}$. Distinct retrofit costs for each option $a \to a'$ allow modeling increasing marginal costs to increasing retrofit depth, reflecting that saving additional energy becomes more expensive as retrofit ambitions grow. The total retrofit expenditures are

$$RETEX = \sum_{y} \left(F_y \sum_{a\to a',d} K^{\mathrm{B}}_{a\to a',d} \Delta n^{\mathrm{B}}_{a\to a',y,d} \right), \tag{7}$$

where F_y denotes the discount factor to the financial base year y_0. The salvage value of a building retrofit depends on the assumed technical lifetime $L^{\mathrm{B}}_{a\to a'}$, the year of investment y, and the time elapsed until the final year of the planning horizon y^{last}. The model assumes that investments underlay linear value decay over their technical lifetime so that the annual salvage value of a building retrofit is

$$v^{\mathrm{B}}_{a\to a',y,d} = K^{\mathrm{B}}_{a\to a',d} \Delta n^{\mathrm{B}}_{a\to a',y,d} \left(1 - \left(\frac{y^{\mathrm{last}} - y + 1}{L^{\mathrm{B}}_{a\to a'}}\right)\right) F_{y^{\mathrm{last}}}, \quad \forall a\to a', y, d \text{ if } y > y^{\mathrm{last}} - L^{\mathrm{B}}_{a\to a'}, \text{ else } 0, \tag{8}$$

and the total salvage value of all building retrofits is

$$v^{\mathrm{B}} = \sum_{a\to a',y,d} v^{\mathrm{B}}_{a\to a',y,d}. \tag{9}$$

3.2.2. Number of heat generation units

The number of HGUBs of type h which were initially installed in a building of archetype a^{I} in a district d in year y is $n^{\mathrm{G}}_{h,a^{\mathrm{I}},y,d}$. The residual number of installed HGUBs $N^{\mathrm{G,res}}_{h,a^{\mathrm{I}},y,d}$ is the number of units that remain available from construction times before the modeling period. The total number of installed HGUBs is then calculated as

$$n^{\mathrm{G}}_{h,a^{\mathrm{I}},y,d} = N^{\mathrm{G,res}}_{h,a^{\mathrm{I}},y,d} + \sum_{\substack{y' \\ y - L^{\mathrm{G}}_h < y' \le y}} n^{\mathrm{G,new}}_{h,a^{\mathrm{I}},y,d}, \quad \forall h, a^{\mathrm{I}}, y, d, \tag{10}$$

where $n^{\mathrm{G,new}}_{h,a^{\mathrm{I}},y,d}$ is the number of newly built HGUBs and L^{G}_h denotes their lifetime. This constraint ensures that no HGUB is retired before reaching the end of its lifetime. The number of HGUBs which are installed in buildings which undergo retrofitting without exchanging the HGUBs is $\Delta n^{\mathrm{G}}_{h,a^{\mathrm{I}},a\to a',y,d}$ where a^{I} denotes the archetype when a HGUB was initially installed and $a \to a'$ specifies the building retrofit. This number is coupled to $\Delta n^{\mathrm{B}}_{a\to a',y,d}$ as

$$\sum_{a^{\mathrm{I}}} \Delta n^{\mathrm{G}}_{h,a^{\mathrm{I}},a\to a',y,d} \le \Delta n^{\mathrm{B}}_{a\to a',y,d}, \quad \forall h, y, d. \tag{11}$$

Note that if a HGUB is exchanged during a building retrofit, then $\Delta n^{\mathrm{G}}_{h,a^{\mathrm{I}},a\to a',y,d} = 0$ and $\Delta n^{\mathrm{B}}_{a\to a',y,d}$ is not. The variable $n^{\mathrm{G}}_{h,a^{\mathrm{I}},a^{\mathrm{OP}},y,d}$ denotes the number of installed HGUBs and additionally indicates the archetype of operation a^{OP}. The joint information of h, a^{I} and a^{OP} enables the correct retirement of HGUBs at the end of their lifetime, even if the archetype of operation changed due to retrofitting. The total number of installed HGUBs does not change due to retrofitting as it is constrained by

$$n^{\mathrm{G}}_{h,a^{\mathrm{I}},y,d} = \sum_{a^{\mathrm{OP}}} n^{\mathrm{G}}_{h,a^{\mathrm{I}},a^{\mathrm{OP}},y,d}, \quad \forall h, a^{\mathrm{I}}, y, d. \tag{12}$$

The total number of HGUBs, including the heat exchangers to connect buildings to the DHN, operating within an archetype a^{OP} must be equal to the total number of buildings of the corresponding archetype in that district, i.e.,

$$\sum_{h,a^{\mathrm{I}}} n^{\mathrm{G}}_{h,a^{\mathrm{I}},a^{\mathrm{OP}},y,d} = n^{\mathrm{B}}_{a^{\mathrm{OP}},y,d}, \quad \forall a^{\mathrm{OP}}, y, d. \tag{13}$$

Changes in the operation of installed HGUBs over the investment years are described by

$$n^{\mathrm{G}}_{h,a^{\mathrm{I}},a^{\mathrm{OP}},y,d} \le n^{\mathrm{G}}_{h,a^{\mathrm{I}},a^{\mathrm{OP}},y-1,d} - \sum_{\substack{a \\ a^{\mathrm{OP}}\to a}} \Delta n^{\mathrm{G}}_{h,a^{\mathrm{I}},a^{\mathrm{OP}}\to a,y,d} + \sum_{\substack{a \\ a\to a^{\mathrm{OP}}}} \Delta n^{\mathrm{G}}_{h,a^{\mathrm{I}},a\to a^{\mathrm{OP}},y,d} + n^{\mathrm{G,new}}_{h,a^{\mathrm{I}},y,d} 1_{[a^{\mathrm{OP}}=a^{\mathrm{I}}]}, \quad \forall h, a^{\mathrm{I}}, a^{\mathrm{OP}}, y, d \text{ if } y > y_0, \tag{14}$$

where $1_{[a^{\mathrm{OP}}=a^{\mathrm{I}}]}$ implies that $n^{\mathrm{G,new}}_{h,a^{\mathrm{I}},y,d}$ is only added to the number of HGUBs if the archetype of operation is equal to the archetype of installation. Through retirement at the end of a HGUB's lifetime the left-hand side can also be less than the term on the right-hand side. Investment costs of HGUBs are specified per installed unit and depend on the archetype where they are installed a^{I}. Archetype buildings representing higher energy standards require less heating power, resulting in reduced investment costs for HGUBs. The costs for a new HGUB in € are $K^{\mathrm{G}}_{h,a^{\mathrm{I}},y,d}$ and are calculated prior to the optimization based on the required heating capacity of the archetype buildings. Then, the total expenditures for HGUBs are

$$GENEX = \sum_{y} \left(F_y \sum_{h,a^{\mathrm{I}},d} K^{\mathrm{G}}_{h,a^{\mathrm{I}},y,d} n^{\mathrm{G,new}}_{h,a^{\mathrm{I}},y,d} \right). \tag{15}$$

Similar to Eq. (8), its annual salvage value is calculated as

$$v^{\mathrm{G}}_{h,a^{\mathrm{I}},y,d} = n^{\mathrm{G,new}}_{h,a^{\mathrm{I}},y,d} K^{\mathrm{G}}_{h,a^{\mathrm{I}},y,d} \left(1 - \left(\frac{y^{\mathrm{last}} - y + 1}{L^{\mathrm{G}}_h}\right)\right) F_{y^{\mathrm{last}}}, \quad \forall h, a^{\mathrm{I}}, y, d \text{ if } y > y^{\mathrm{last}} - L^{\mathrm{G}}_h, \text{ else } 0, \tag{16}$$

and the total salvage value of all newly installed HGUBs is

$$v^{\mathrm{G}} = \sum_{h,a^{\mathrm{I}},y,d} v^{\mathrm{G}}_{h,a^{\mathrm{I}},y,d}. \tag{17}$$

The binary variable $u_{\theta,y,d}$ indicates whether a DHN operates at a temperature θ. The DHN can only be operated at one temperature in a year and district, so that

$$\sum_{\theta} u_{\theta,y,d} \le 1, \quad \forall y, d. \tag{18}$$

3.3. Coupling

Coupling conditions integrate the number-based constraints into the existing ESM framework. They differ from the other conditions by also relying on variables which are part of the already existing ESM framework. Four of the five coupling conditions are used to limit the total yearly energy output of selected conversion processes, $e^{\mathrm{outtot}}_{c,y,d}$, following Eq. (2). In an OSeMOSYS model, this would correspond to constraining the total annual activity of a technology. The fifth coupling condition introduces additional cost terms to the objective function.

The total heat demand of all buildings of one archetype is the product of the number of buildings per archetype $n^{\mathrm{B}}_{a,y,d}$ and the annual demand of one building of that respective archetype $D_{a,y,d}$. The set Υ contains pairs of conversion processes and corresponding archetype buildings. By constraining

$$e^{\mathrm{outtot}}_{c,y,d} = n^{\mathrm{B}}_{a,y,d} D_{a,y,d}, \quad \forall y, d, \ (c,a) \in \Upsilon, \tag{19}$$

the heat demand of the buildings can be represented while accounting for building retrofits. To avoid cooperation of HGUBs, the total yearly energy output of conversion processes representing HGUBs is constrained by

$$e^{\mathrm{outtot}}_{c,y,d} = \sum_{\substack{a^{\mathrm{I}} \\ a^{\mathrm{OP}} \ge a^{\mathrm{I}}}} n^{\mathrm{G}}_{h,a^{\mathrm{I}},a^{\mathrm{OP}},y,d} D_{a^{\mathrm{OP}},y,d}, \quad \forall y, d, \ (c,h,a^{\mathrm{OP}}) \in \Psi, \tag{20}$$

where Ψ contains triples of conversion processes and the corresponding HGUB they represent.

The objective function of the CESM framework minimizes total system expenditures $TOTEX$ as the sum of investment expenditures $CAPEX$ and operational expenditures $OPEX$, minus investment salvage values v^{C}. The objective function is extended to include retrofitting expenditures $RETEX$, HGUB expenditures $GENEX$, and their respective salvage values v^{B} and v^{G}, so that

$$\begin{aligned} TOTEX =& CAPEX + OPEX + RETEX + GENEX \\ & - v^{C} - v^{G} - v^{B}, \end{aligned} \tag{21}$$

where the salvage values represent the remaining value of investments that have not yet reached the end of their technical lifetime by the end of the modeling period.

The set Ω contains pairs of conversion processes c which are supplied by the DHN, such as heat exchangers that connect individual buildings or connections to neighboring DHNs, and their required minimum temperature θ. For example, a heat exchanger serving an archetype building with a low energy standard can only be supplied by the DHN if the network operates at a sufficiently high temperature. Such a conversion process can only be supplied by the DHN if the DHN operates at temperature θ or higher, which is ensured by constraining

$$e^{\text{outtot}}_{c,y,d} \leq M \sum_{\substack{\theta' \\ \theta \leq \theta'}} u_{\theta',y,d}, \quad \forall y, d, (c,\theta) \in \Omega, \tag{22}$$

where M is a sufficiently large constant, exceeding the maximum possible heat demand within a district. Conversely, if a DHN operates at temperature θ', it can only receive heat from HGUCs supplying θ' or higher temperatures. The set Γ contains pairs of conversion processes c supplying the DHN, such as the HGUCs, and the temperature θ they supply, so that

$$e^{\text{outtot}}_{c,y,d} \leq M \sum_{\substack{\theta' \\ \theta' \leq \theta}} u_{\theta',y,d}, \quad \forall y, d, (c,\theta) \in \Gamma. \tag{23}$$

The set Ω captures the relationship between archetypes and the required heat supply temperature when buildings are connected to a DHN. For individual heat supply via HGUB, temperature levels are captured implicitly, for example through higher HP efficiencies in retrofitted buildings.

3.4. Summary

This section outlined the approach to enhance existing ESM frameworks to enable the modeling of interdependencies between heat supply-side and demand-side measures at an urban scale. Eqs. (3) to (18) describe the new number-based conditions and Eqs. (19) to (23) integrate these into the existing ESM framework.

The approach allows addressing the limitations of many ESM frameworks arising from the lack of a one-to-one assignment between heat demands and supplies (Section 2.2). By (i) defining distinct conversion processes for each HGUB h supplying a specific archetype a, and by (ii) calculating costs of HGUBs based on numbers instead of capacities, investment costs are not skewed by the aggregation of different heat demands. This also allows the use of non-linear cost functions for HGUBs without introducing additional binary variables or compromising the MILP structure of the optimization problem. (iii) By constraining the load shape of each HGUB's energy output to align with the demand profile of the building it serves and by (iv) constraining the total yearly energy outputs of HGUBs to the demand of the supplied buildings, the HGUBs cannot cooperate to meet the total heat demands. (v) The conditions presented in this work ensure that this holds even when building retrofits are modeled endogenously.

Binary variables are only used to model the DHNs. To model investment costs independently of the installed capacity, a binary variable is used for every district and investment year. This binary variable is already part of many existing ESM frameworks. Furthermore, a new binary variable $u_{\theta,y,d}$ is introduced for every possible operation temperature of a DHN, district and investment year. With $\sum_{\theta} u_{\theta,y,d} \leq 1$, the maximum number of binaries of the energy system model, including the binaries to model the fixed investment costs, is $N_d N_y N_\theta$, where N_d is the number of districts, N_y is the number of investment years and N_θ is the number of possible temperatures of a DHN. Given that these numbers are generally limited to small values at urban scales, this ensures reasonable solving times even for large problem instances.

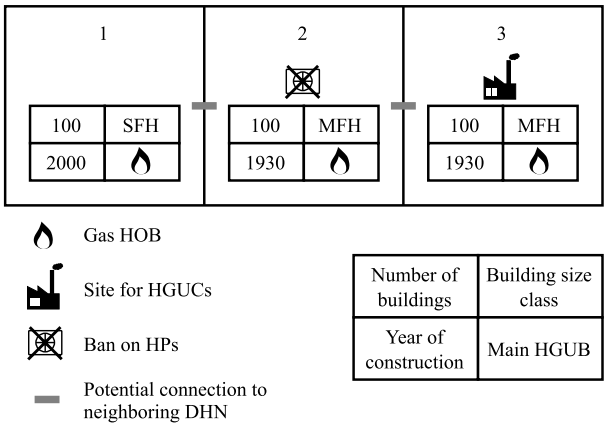

Fig. 5. Layout of the fictive urban area.

4. Experimental case study

This section presents a case study of a fictive urban area consisting of three districts. Each district is characterized by common urban building types with their respective heating systems, encompassing a newly developed district with single family houses (SFHs) supplied by HPs and older districts with multi family houses (MFHs) supplied by gas HOBs. The CESM framework introduced in Section 2 is extended with the conditions outlined in Section 3, and the impact of these conditions is evaluated by comparing the results of the *base scenario*, which incorporates the proposed conditions, to two alternative scenarios. The *no waste heat scenario* illustrates how the absence of central heat sources can significantly influence the optimal heat supply structure and retrofit decisions within an urban area. The *fixed retrofit rate scenario* assumes heat demand reductions through predefined retrofit rates, a common assumption in ESM, and serves as a benchmark to evaluate the potential of the proposed approach which models retrofit decisions endogenously.

The optimization aims for the cost-optimal decarbonization of the residential heat sector by 2045, assuming full decarbonization of the electricity sector by the same year to enable this transition. There are five investment years evenly distributed from 2025 until 2045. The first year of the modeling period, 2025, represents the initial state of the urban area, during which no investments can be made. An interest rate of 3 % is assumed.

4.1. Setup

The layout of the urban area, including potential connections between neighboring DHNs and the most important characteristics of the districts, are shown in Fig. 5. The districts vary in their archetype buildings, the availability of HGUCs, or the number of residual HGUBs which define the heat supply structure in the initial modeling year 2025. In every district there are 100 buildings. Detailed input data is outlined in the Appendix.

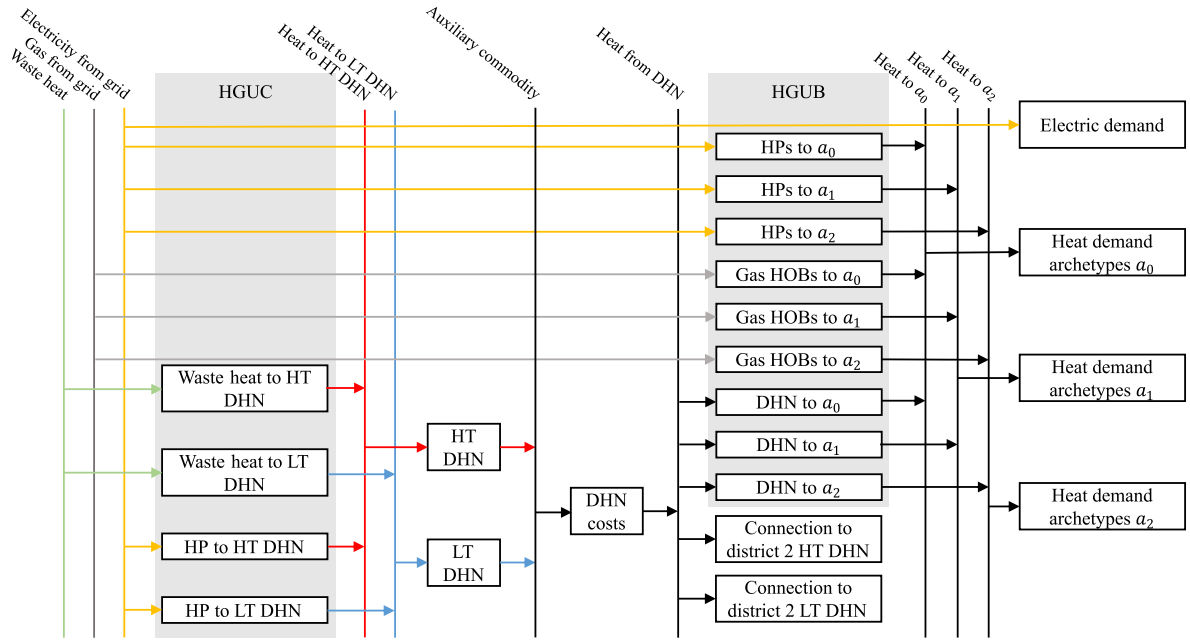

Fig. 6. Model structure of district 3.

Table 2
Archetype buildings by district and their minimum required heat supply temperatures.

	District			Minimum required supply temperature
	1	2	3	
Low energy standard a_0		x	x	HT
Medium energy standard a_1	x	x	x	LT
High energy standard a_2	x	x	x	LT

Central heat supply. In each district, a DHN can be constructed and operated at either HT, corresponding to a 3rd Generation District Heating system with supply temperatures between 70 °C and 100 °C, or LT, corresponding to a 4GDH with temperatures between 50 °C and 70 °C and higher energy efficiency [5].

If a DHN operates at LT, grid losses are reduced compared to those of a HT DHN. If two DHNs of the same temperature are established in neighboring districts, heat can be exchanged between them. Additionally, heat can be transferred from a district with a HT DHN to a district with a LT DHN, but not in the reverse direction. The model structure of district 3 is depicted in Fig. 6. HGUCs are restricted to installation in district 3 due to zoning regulations that prohibit their deployment in other districts. Central HPs are more efficient when supplying LT heat compared to HT heat. A waste heat source with a maximum capacity of 1.5 MW is available. The waste heat source is assumed to provide LT heat, making it more cost-effective to supply a LT DHN compared to a HT DHN. Supplying a HT DHN would require an additional HP to raise the waste heat temperature, resulting in higher costs.

Archetype buildings. For each district, archetype buildings are defined, differing in heat and electricity demand. In this model, each district contains a single *type* of building, defined by the construction year, area and the building size class (e.g. SFH or MFH), while the archetypes within a district represent varying energy standards of that building type. Across all districts, an archetype a_0 corresponds to a low energy standard, a_1 to a medium energy standard, and a_2 to a high energy standard. All archetypes can potentially be supplied by a HT DHN, but only a_1 and a_2 can be supplied by a LT DHN. Table 2 provides an overview of the different archetype buildings in each district. In districts 2 and 3 each, three archetype buildings, a_0, a_1, and a_2, are defined. Consequently, the following retrofits are possible: $a_0 \rightarrow a_1$, $a_1 \rightarrow a_2$, and $a_0 \rightarrow a_2$. For district 1, only two archetype buildings, a_1 and a_2, are defined. Since the buildings in district 1 were built in year 2000, their unretrofitted state already corresponds to a medium energy standard. Therefore, the only possible retrofit in this district is $a_1 \rightarrow a_2$.

Table 3
Results of the case study.

	Base scenario	No waste heat scenario	Fixed retrofit rate scenario
$TOTEX$ [Mio €]	16.76	17.92	18.69
Comparison to base scenario	+0 %	+6.9 %	+11.5 %
DHN temperature	LT	LT	HT
Main heat supply in district 3 in 2045	DHN	HP	HP
Total heat demand	226 GWh	238 GWh	234 GWh
Retrofit rate overall			
2030	2.0 %	1.0 %	2.0 %
2035	2.0 %	1.0 %	2.0 %
2040	2.0 %	1.5 %	2.0 %
2045	2.0 %	1.8 %	2.0 %
Retrofit rate district 1			
2030	0.0 %	0.0 %	2.0 %
2035	0.0 %	0.0 %	2.0 %
2040	0.0 %	0.0 %	2.0 %
2045	0.0 %	0.0 %	2.0 %
Retrofit rate district 2			
2030	3.0 %	3.0 %	2.0 %
2035	3.0 %	3.0 %	2.0 %
2040	3.0 %	3.0 %	2.0 %
2045	3.0 %	3.0 %	2.0 %
Retrofit rate district 3			
2030	3.0 %	0.0 %	2.0 %
2035	3.0 %	0.0 %	2.0 %
2040	3.0 %	1.6 %	2.0 %
2045	3.0 %	2.4 %	2.0 %

The yearly heat demand for the archetype buildings is derived from the TABULA Webtool, which ensures thermal comfort by maintaining an indoor air temperature of 20 °C [32]. Load profiles are generated using the oemof *demandlib* module [9]. Retrofit costs are estimated based on [33]. Detailed input data can be found in the Appendix.

The maximum retrofit rate is 2 % per year across the entire urban area. Since the retrofit rate is limited for the entire urban area, certain

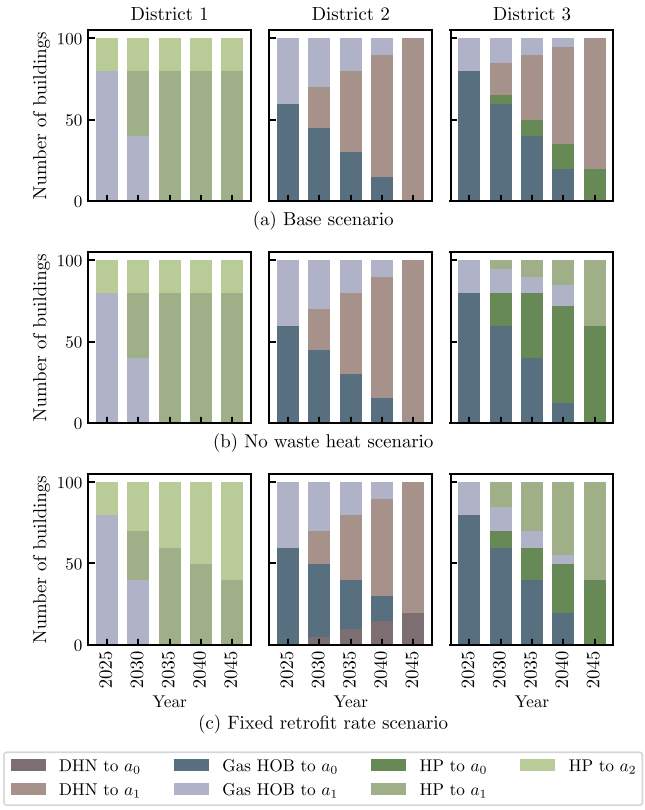

Fig. 7. Optimal heat supply structure of the three districts.

districts may exhibit higher retrofit rates at the expense of lower rates in others. No minimum retrofit rate is enforced, as building retrofit is assumed to be purely cost-driven.

Individual heat supply. Individual heat supply can be provided either through gas HOBs or HPs. Additionally, heat exchangers connecting the buildings to the DHN are modeled as HGUBs. The efficiency of HPs depends on the energy standard of the supplied building. As the energy standard improves, the required heat supply temperature decreases, leading to higher HP efficiencies. In district 2, located in the city center, the high building density constrains the use of individual HPs. Therefore, the decarbonization strategy for this district is restricted to a DHN.

In the first year of the modeling period, all buildings are initially supplied by individual gas HOBs, except in district 1, where 20 buildings of the highest energy standard a_2 are supplied by HPs. Details regarding the initial supply structure of the buildings and the number of residual HGUBs are provided in the Appendix.

Scenarios. The described setting constitutes the *base scenario* of the case study. The *no waste heat scenario* examines how the absence of the waste heat source influences the optimization results, with a particular focus on the optimal retrofit decisions, to investigate the necessity of modeling supply–demand interdependencies endogenously. Finally, the *fixed retrofit rate scenario* assumes a constant retrofit rate of 2 % per year and across all districts, a common assumption in ESM when building retrofits are not considered endogenously, and serves as a benchmark for the presented approach.

The case study model comprises 538 543 equations and 458 676 variables of which 30 are binary. Using CPLEX 22.1.1 [34] with a zero MIP gap tolerance, all scenarios are solved in under a minute on a standard laptop, accounting for 224 representative time steps per investment year.

4.2. Results base scenario

The optimal heat supply structure for decarbonizing the urban area under consideration in the base scenario is illustrated in Fig. 7a. In district 1, where buildings are already of medium or high energy standards, no retrofits are carried out. Retiring gas HOBs are replaced by HPs. In district 2, individual HPs are not permitted due to spatial constraints associated with the high density of buildings. Consequently, as gas HOBs reach the end of their technical lifetime, they are replaced by heat exchangers to connect the buildings to the DHN. By 2045, all buildings in district 2 are connected to the DHN.

The development of the DHN in district 2 necessitates the construction of a DHN in district 3, as suitable locations for HGUCs are only available in district 3. As gas HOBs in district 3 reach the end of their technical lifetime, their replacement strategy depends on the energy standard of the respective building. Buildings of medium energy standard a_1 are connected to the DHN while buildings of the lowest energy standard a_0 are supplied by a HP, as connecting them to the DHN would necessitate an increase of the supply temperature of the entire DHN. Instead, the DHN operates at LT over the whole modeling period, thereby minimizing distribution losses. This is enabled by annual retrofit rates of 3 % in districts 2 and 3. Since no retrofitting occurs in district 1, the overall retrofit rate for the entire urban area remains within the 2 % limit.

There are two reasons why buildings are retrofitted from the lowest to the medium energy standard, but not to the highest energy standard a_2. First, building retrofit is subject to increasing marginal costs to increasing retrofit depth, i.e., the higher the energy saving ambition, the higher the costs to save one additional unit of energy [33]. Second, in this case study, the benefits from interdependencies between DHN heat supply and building retrofits are identical for retrofits to either a_1 or a_2, since LT heat can supply buildings of medium (a_1) and high energy (a_2) standards.

Fig. 8a shows a declining heat demand over the modeling period due to building retrofits. As tightening CO_2-limits necessitate investments in more expensive technologies, Fig. 8b shows increasing levelized cost of heating (LCOH), defined as the annual average cost per kWh of heat. The LCOH include annual operational costs $OPEX$, excluding those for residential electricity demand, as well as annuitized investment expenditures $CAPEX$, $GENEX$ and $RETEX$ over the respective lifetimes.

Fig. 9 shows that HGUCs cooperate to supply heat to the DHN. Peak loads that cannot be supplied by the waste heat because of capacity limitations are covered by a HP. Fig. 10 shows the power output of the gas HOB and the DHN to supply heat to the archetype buildings a_1 in district 3 for one week in December 2035. By constraining both the shape (Eq. (1)) and the amount (Eq. (20)) of the energy output to exactly match the heat demand, the different HGUBs cannot cooperate to meet the total heat demand.

4.3. No waste heat scenario

This scenario investigates the necessity of modeling supply–demand interdependencies endogenously by examining how the availability of heat sources (supply-side) influences retrofit decisions (demand-side). Compared to the base scenario, this scenario differs solely in the absence of a waste heat source in district 3. The reduction in available heat sources for the DHN results in a shift in optimal retrofit decisions, as detailed in Table 3. The resulting optimal heat supply structure is illustrated in Fig. 7b. Buildings in district 2 are retrofitted to enable LT heat supply via the DHN, benefiting of reduced heat losses and an increased efficiency of central HPs. In contrast, in district 3, only a limited number of buildings are retrofitted in 2040 and 2045. In district 3, individual heat supply is favored over connecting buildings to the DHN via heat exchangers. Gas HOBs at the end of their lifetime are gradually replaced with new HPs, as the absence of a waste heat source

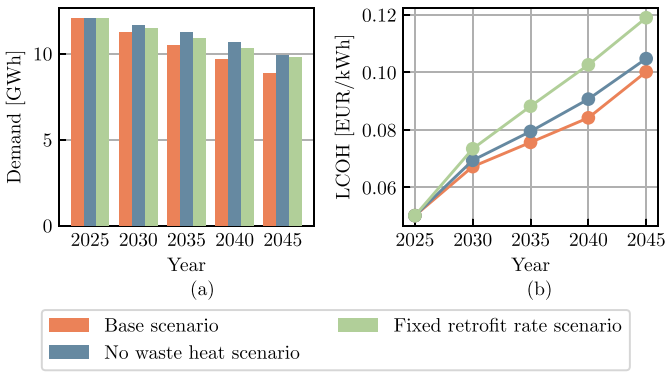

Fig. 8. Evolution of (a) the annual heat demands and (b) the LCOH of the entire urban area during the modeling period.

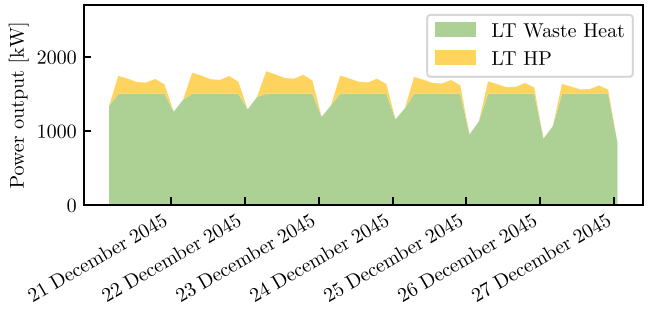

Fig. 9. Power output of HGUCs to supply heat to the DHN in district 3 in year 2045 in the base scenario.

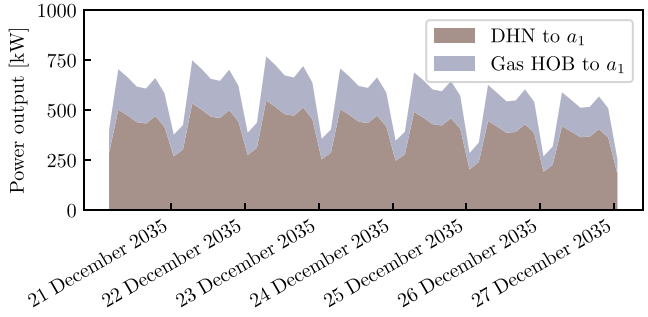

Fig. 10. Power output to the buildings of archetype a_1 in district 3 in year 2035 in the base scenario.

increases the cost of centralized heat generation, making individual heat supply the more cost-effective alternative. Overall, compared to the base scenario, total system costs rise by 6.9 %.

This scenario analysis shows that the availability of heat sources can significantly influence the optimal heat supply structure and retrofit decisions within an urban area.

4.4. Fixed retrofit rate scenario

In the fixed retrofit rate scenario, the model is constrained to retrofit 2.0 % of the buildings per district and year. The resulting optimal heat supply structure is illustrated in Fig. 7c. Due to the fixed retrofit rate, not all buildings in district 2 can be retrofitted to at least a medium energy standard a_1 by 2045. Consequently, the system is forced to operate the DHN at HT to ensure the decarbonization of heat supply in district 2.

Similar to the *no waste heat scenario*, individual heat supply is preferred over central heat supply in district 3. This preference arises from the necessity of operating the DHN at HT, which increases centralized heat generation costs, making individual heat supply the more economical option.

Compared to the base scenario, total system costs increase by 11.5 %. This cost increase is driven by two factors. First, the requirement to operate the DHN at HT results in higher thermal losses, increased costs for waste heat, and reduced efficiency of the central HP supplying the DHN. Second, the fixed retrofit rate applies uniformly across all districts, enforcing building retrofits in district 1. In contrast, in the other scenarios, no retrofits occurred in district 1, as the buildings there already met medium or high energy standards. As discussed in Section 4.2, building retrofits to the highest energy standard a_2 are not cost-optimal in this setting. This is also reflected in Fig. 8a, where the heat demand decreases less than in the base scenario, despite the same number of building retrofits. As a result of the high investment costs, this scenario shows the highest LCOH among all scenarios (see Fig. 8b).

This scenario analysis shows that relying on predefined retrofit rates and heat demand reductions can lead to suboptimal decisions compared to the endogenous modeling proposed in this work, as it may overlook potential synergies between heat supply and demand.

5. Conclusion

This work proposed new conditions to extend existing ESM frameworks to identify optimal decarbonization paths of the urban residential heating sector modeling supply–demand interdependencies endogenously. By extending ESM frameworks with the proposed conditions, limitations in their application for urban-scale modeling due to a missing one-to-one assignment of demands and supplies can be overcome. In the proposed approach, the optimal energy system design is not only determined by the installed capacities of HGUBs, but also by the number of buildings of a certain archetype that are supplied by a particular HGUB within a district and year. The number-based modeling of the heat supply enables the endogenous modeling of building retrofits while representing important characteristics of the heating sector.

The results demonstrate that the location and availability of heat sources influence the optimal retrofit strategy, supporting the claim that supply–demand interdependencies should be considered simultaneously. The benchmark scenario, which assumes a predefined constant retrofit rate uniformly distributed across the urban area, is 11.5 % more expensive than results obtained with the proposed conditions. By leveraging existing synergies, modeling supply–demand interdependencies endogenously can enhance the cost efficiency of heating systems.

While the proposed approach offers valuable insights, several limitations should be addressed before real-world application. It is best suited for urban areas divisible into districts with relatively homogeneous building stocks. Highly heterogeneous areas require many archetypes per district, reducing accuracy under the assumption of a continuous number of buildings. Key inputs, such as building energy standards and retrofit costs, are often uncertain and difficult to obtain. The model's sensitivity to these parameters should be assessed before practical application. The method's efficient computation times enable extensive scenario analyses to address long-term uncertainties, such as fuel prices and waste heat availability, which should be examined in real-world applications. Although promising, the method's scalability to an urban area with hundreds of districts has yet to be validated. Future extensions should incorporate additional technologies, e.g., booster HPs [35], more detailed heat demand simulations [36], and address stakeholder behavior, such as homeowners' retrofit decisions and the incentives that influence them.

In summary, this work enables the identification of optimal building-level solutions within the broader context of the urban heating system. Via the five coupling conditions, the proposed method is highly flexible and can be used to enhance a wide range of existing energy system models. Applying this approach can support municipal policymakers identify target areas for individual heat supply and DHNs, enabling targeted incentives to cost-optimally decarbonize the urban heating system by aligning individual retrofit decisions and heating system upgrades with energy providers' DHN expansion plans.

Table A.4
Characteristics of the archetype buildings derived from the TABULA Webtool [32,37]. The electricity demand is estimated by multiplying the net area by a factor of 30 kWh/m^2.

District ID	Building size class	Construction year	Net area [m^2]	Heat demand a_0 [MWh/a]	Heat demand a_1 [MWh/a]	Heat demand a_2 [MWh/a]	Electricity demand [MWh/a]
1	SFH	2000	122	–	13.1	7.8	3.7
2	MFH	1930	385	62.1	35.6	20.1	11.6
3	MFH	1930	385	62.1	35.6	20.1	11.6

Table A.5
Retrofit costs for each district. For the advanced retrofit $a_0 \rightarrow a_2$ costs of 175 €/m^2 are assumed based on the costs of retrofit package 10 in Germany in [33]. Since [33] accounts for gross areas, whereas the TABULA Webtool [32,37] indicates net areas, an additional 20 % was added to the retrofit costs. The retrofits $a_0 \rightarrow a_1$ and $a_1 \rightarrow a_2$ each cost 50 % of the $a_0 \rightarrow a_2$ retrofit.

District ID	Retrofit costs $a_0 \rightarrow a_1$ [€]	Retrofit costs $a_1 \rightarrow a_2$ [€]	Retrofit costs $a_0 \rightarrow a_2$ [€]
1	–	13 200	–
2	40 800	40 800	81 600
3	40 800	40 800	81 600

Table A.6
Technical specifications of HGUBs.

Name	Lifetime [a]	Input commodity	Output commodity	Efficiency	Investment costs fixed [€]	Investment costs variable [€/kW]
Gas HOB	20	Gas	Heat	0.99	5000	110
HP	20	Electricity	Heat	a_0: 2.5[a]	2023: 6000[b]	2023: 1200[b]
				a_1: 3.0[a]	2030: 5700[b]	2030: 1100[b]
				a_2: 3.5[a]	2040: 5000[b]	2040: 1000[b]
Heat exchangers	25	Heat from DHN	Heat	1	10 000	200

[a] The efficiency of the HP depends on the energy standard of the supplied building.
[b] Decreasing costs due to technology improvements are assumed over the modeling period. For investment years which are not listed the costs are linearly interpolated.

CRediT authorship contribution statement

Carolin Ayasse: Writing – original draft, Visualization, Validation, Software, Methodology, Investigation, Data curation, Conceptualization. **Julia Barbosa:** Writing – review & editing, Methodology, Conceptualization. **Florian Steinke:** Writing – review & editing, Supervision, Resources, Methodology, Funding acquisition, Conceptualization.

Declaration of Generative AI and AI-assisted technologies in the writing process

During the preparation of this work the author(s) used ChatGPT in order to improve the clarity and readability. After using this tool/service, the author(s) reviewed and edited the content as needed and take(s) full responsibility for the content of the publication.

Declaration of competing interest

The authors declare that they have no known competing financial interests or personal relationships that could have appeared to influence the work reported in this paper.

Acknowledgments

This work was supported by the project executing agency Jülich (PTJ) with funds provided by the German Federal Ministry for Economic Affairs and Climate Action (BMWK) [grant number 03EN3077A].

Appendix. Case study data

See Tables A.4, A.5, A.6, A.7, A.8, A.9, A.10.

Data availability

Data will be made available on request.

References

[1] European Commission and Directorate-General for Energy, Braungardt S, Bürger V, Fleiter T, Bagheri M, Manz P, Billerbeck A, Al-Dabbas K, Breitschopf B, Winkler J, Fallahnejad M, Harringer D, Hasani J, Kök A, Kranzl L, Mascherbauer P, Hummel M, Müller A, Habiger J, Persson U, Sánchez-García L. Renewable heating and cooling pathways – Towards full decarbonisation by 2050 – Final report. Publications Office of the European Union; 2023, http://dx.doi.org/10.2833/036342.
[2] European Commission. Energy performance of buildings directive. 2024.
[3] Brozovsky J, Gustavsen A, Gaitani N. Zero emission neighbourhoods and positive energy districts – A state-of-the-art review. Sustain Cities Soc 2021;72:103013. http://dx.doi.org/10.1016/j.scs.2021.103013.
[4] European Commission. Energy efficiency directive. 2023.
[5] Lund H, Werner S, Wiltshire R, Svendsen S, Thorsen JE, Hvelplund F, Mathiesen BV. 4Th generation district heating (4GDH). Energy 2014;68:1–11. http://dx.doi.org/10.1016/j.energy.2014.02.089.
[6] Lund H, Østergaard PA, Chang M, Werner S, Svendsen S, Sorknæ s P, Thorsen JE, Hvelplund F, Mortensen BOG, Mathiesen BV, Bojesen C, Duic N, Zhang X, Möller B. The status of 4th generation district heating: Research and results. Energy 2018;164:147–59. http://dx.doi.org/10.1016/j.energy.2018.08.206.
[7] IEA-ETSAP. TIMES model generator. 2025, http://dx.doi.org/10.5281/ZENODO.3865460.
[8] Howells M, Rogner H, Strachan N, Heaps C, Huntington H, Kypreos S, Hughes A, Silveira S, DeCarolis J, Bazillian M, Roehrl A. OSeMOSYS: the open source energy modeling system. Energy Policy 2011;39(10):5850–70. http://dx.doi.org/10.1016/j.enpol.2011.06.033.
[9] Hilpert S, Kaldemeyer C, Krien U, Günther S, Wingenbach C, Plessmann G. The open energy modelling framework (oemof) - A new approach to facilitate open science in energy system modelling. Energy Strat Rev 2018;22:16–25. http://dx.doi.org/10.1016/j.esr.2018.07.001.
[10] Hajikazemi S, Barbosa J. Compact energy system modeling tool (CESM). 2024, http://dx.doi.org/10.5281/zenodo.13902515.
[11] Nagy Z, Rossi D, Hersberger C, Irigoyen SD, Miller C, Schlueter A. Balancing envelope and heating system parameters for zero emissions retrofit using building sensor data. Appl Energy 2014;131:56–66. http://dx.doi.org/10.1016/j.apenergy.2014.06.024.
[12] Delmastro C, Gargiulo M. Capturing the long-term interdependencies between building thermal energy supply and demand in urban planning strategies. Appl Energy 2020;268:114774. http://dx.doi.org/10.1016/j.apenergy.2020.114774.
[13] Wu R, Mavromatidis G, Orehounig K, Carmeliet J. Multiobjective optimisation of energy systems and building envelope retrofit in a residential community. Appl Energy 2017;190:634–49. http://dx.doi.org/10.1016/j.apenergy.2016.12.161.

Table A.7
Technical specifications of HGUCs.

Name	Lifetime [a]	Input commodity	Output commodity	Efficiency	Investment costs [€/kW]	Operational costs [€/MWh]
HP to HT DHN	25	Electricity	Heat to HT DHN	3	900	0
HP to LT DHN	25	Electricity	Heat to LT DHN	3.5	900	0
Waste heat to HT DHN	25	Waste heat	Heat to HT DHN	1	0	15
Waste heat to LT DHN	25	Waste heat	Heat to LT DHN	1	0	45

Table A.8
Residual number of HGUBs $N^{\mathrm{G,res}}_{h,a^{\mathrm{I}},y,d}$.

District ID	HGUB	2025	2030	2035	2040	2045
1	Gas HOB a_1	80	40	0	0	0
1	HP a_2	20	15	10	5	0
2	Gas HOB a_0	60	45	30	15	0
2	Gas HOB a_1	40	30	20	10	0
3	Gas HOB a_0	80	60	40	20	0
3	Gas HOB a_1	20	15	10	5	0

Table A.9
Technical specifications of the DHN.

Lifetime	Costs [Mio €]	Efficiency HT DHN	Efficiency LT DHN
25	1	0.7	0.85

Table A.10
Technical specifications of energy imports.

Commodity	Costs [€/MWh]	CO_2-emission [t/MWh]	Max. capacity [MW]
Gas	50	0.2	–
Electricity	100	2020: 0.26[a] 2045: 0.00[a]	–
Waste heat	–	0	1.5

[a] For investment years which are not listed the emissions are linearly interpolated.

[14] Dochev I, Peters I, Seller H, Schuchardt GK. Analysing district heating potential with linear heat density. A case study from Hamburg. Energy Procedia 2018;149:410–9. http://dx.doi.org/10.1016/j.egypro.2018.08.205.

[15] Zhang H, Zhou L, Huang X, Zhang X. Decarbonizing a large City's heating system using heat pumps: A case study of Beijing. Energy 2019;186:115820. http://dx.doi.org/10.1016/j.energy.2019.07.150.

[16] Lund H, Thellufsen JZ, Østergaard PA, Sorknæs P, Skov IR, Mathiesen BV. EnergyPLAN – Advanced analysis of smart energy systems. Smart Energy 2021;1:100007. http://dx.doi.org/10.1016/j.segy.2021.100007.

[17] Akhatova A, Kranzl L. Agent-based modelling of building retrofit adoption in neighbourhoods. Energy Build 2025;328:115172. http://dx.doi.org/10.1016/j.enbuild.2024.115172.

[18] Talbi E-G. Metaheuristics: from design to implementation. 1st ed. Wiley; 2009, http://dx.doi.org/10.1002/9780470496916.

[19] Waibel C, Evins R, Carmeliet J. Co-simulation and optimization of building geometry and multi-energy systems: Interdependencies in energy supply, energy demand and solar potentials. Appl Energy 2019;242:1661–82. http://dx.doi.org/10.1016/j.apenergy.2019.03.177.

[20] National Renewable Energy Laboratory. EnergyPlus. 2025.

[21] Fonseca JA, Nguyen T-A, Schlueter A, Marechal F. City energy analyst (CEA): Integrated framework for analysis and optimization of building energy systems in neighborhoods and city districts. Energy Build 2016;113:202–26. http://dx.doi.org/10.1016/j.enbuild.2015.11.055.

[22] Ascione F, Bianco N, Mauro GM, Napolitano DF. Knowledge and energy retrofitting of neighborhoods and districts. A comprehensive approach coupling geographical information systems, building simulations and optimization engines. Energy Convers Manage 2021;230:113786. http://dx.doi.org/10.1016/j.enconman.2020.113786.

[23] Thrampoulidis E, Hug G, Orehounig K. Approximating optimal building retrofit solutions for large-scale retrofit analysis. Appl Energy 2023;333:120566. http://dx.doi.org/10.1016/j.apenergy.2022.120566.

[24] Mavromatidis G, Petkov I. MANGO: A novel optimization model for the long-term, multi-stage planning of decentralized multi-energy systems. Appl Energy 2021;288:116585. http://dx.doi.org/10.1016/j.apenergy.2021.116585.

[25] Lerbinger A, Petkov I, Mavromatidis G, Knoeri C. Optimal decarbonization strategies for existing districts considering energy systems and retrofits. Appl Energy 2023;352:121863. http://dx.doi.org/10.1016/j.apenergy.2023.121863.

[26] Saad Hussein N. A method for evaluating building retrofit effects on a decentral energy system by a sector coupling operation and expansion model. Energy Syst 2018;9(3):605–45. http://dx.doi.org/10.1007/s12667-017-0257-5.

[27] Iturriaga E, Campos-Celador Á, Terés-Zubiaga J, Aldasoro U, Álvarez-Sanz M. A MILP optimization method for energy renovation of residential urban areas: Towards zero energy districts. Sustain Cities Soc 2021;68:102787. http://dx.doi.org/10.1016/j.scs.2021.102787.

[28] Pavičević M, Novosel T, Pukšec T, Duić N. Hourly optimization and sizing of district heating systems considering building refurbishment – Case study for the city of Zagreb. Energy 2017;137:1264–76. http://dx.doi.org/10.1016/j.energy.2017.06.105.

[29] Jennings M, Fisk D, Shah N. Modelling and optimization of retrofitting residential energy systems at the urban scale. Energy 2014;64:220–33. http://dx.doi.org/10.1016/j.energy.2013.10.076.

[30] Murray P, Marquant J, Niffeler M, Mavromatidis G, Orehounig K. Optimal transformation strategies for buildings, neighbourhoods and districts to reach CO2 emission reduction targets. Energy Build 2020;207:109569. http://dx.doi.org/10.1016/j.enbuild.2019.109569.

[31] Barbosa J, Ripp C, Steinke F. Accessible modeling of the german energy transition: An open, compact, and validated model. Energies 2021;14(23):8084. http://dx.doi.org/10.3390/en14238084.

[32] Loga T, Stein B, Diefenbach N. TABULA building typologies in 20 European countries—Making energy-related features of residential building stocks comparable. Energy Build 2016;132:4–12. http://dx.doi.org/10.1016/j.enbuild.2016.06.094.

[33] Hummel M, Büchele R, Müller A, Aichinger E, Steinbach J, Kranzl L, Toleikyte A, Forthuber S. The costs and potentials for heat savings in buildings: Refurbishment costs and heat saving cost curves for 6 countries in Europe. Energy Build 2021;231:110454. http://dx.doi.org/10.1016/j.enbuild.2020.110454.

[34] IBM ILOG CPLEX Division. CPLEX 22.1.1.0 user's manual. 2022.

[35] Østergaard PA, Andersen AN. Booster heat pumps and central heat pumps in district heating. Appl Energy 2016;184:1374–88. http://dx.doi.org/10.1016/j.apenergy.2016.02.144.

[36] Zhai X, Li Z, Li Z, Xue Y, Chang X, Su J, Jin X, Wang P, Sun H. Risk-averse energy management for integrated electricity and heat systems considering building heating vertical imbalance: An asynchronous decentralized approach. Appl Energy 2025;383:125271. http://dx.doi.org/10.1016/j.apenergy.2025.125271.

[37] Institut Wohnen und Umwelt GmbH. TABULA WebTool. 2025.